ISSN: 0067-2904

Linear and Non-Linear Stability Analysis for Thermal Convection in A Bidispersive Porous Medium with Thermal Non-Equilibrium Effects

Israa Mkheilef Mankhi*, Shatha Ahmed Haddad
Department of Mathematics, College of Sciences, University of Basrah, Basrah, Iraq

Received: 23/5/2021 Accepted: 27/7/2021

Abstract

The linear instability and nonlinear stability analyses are performed for the model of bidispersive local thermal non-equilibrium flow. The effect of local thermal non-equilibrium on the onset of convection in a bidispersive porous medium of Darcy type is investigated. The temperatures in the macropores and micropores are allowed to be different. The effects of various interaction parameters on the stability of the system are discussed. In particular, the effects of the porosity modified conductivity ratio parameters, Γ_p and Γ_s, with the inter-phase momentum transfer parameters μ_1 and μ_2, on the onset of thermal Convection are also considered. Furthermore, the nonlinear stability boundary is found to be below the linear instability threshold. The numerical results are presented for free-free boundary conditions.

Keywords: Bidispersive porous medium, Local thermal non-equilibrium, Linear instability, Nonlinear stability, Darcy model.

تحليل الاستقرار الخطي وغير الخطي للحمل الحراري في وسط ثنائي المسام مع تأثير غير متزن حراريا

إسراء مخيلف منخي*, شذى أحمد حداد
قسم الرياضيات، كلية العلوم، جامعة البصرة، البصرة، العراق

الخلاصة

تم تنفيذ عدم الاستقرار الخطي والاستقرار الخطي لنموذج ثنائي المسام وغير متزن حرارياً. تمت دراسة تأثير عدم الأتزان على بداية الحمل الحراري في وسط ثنائي المسام حيث استخدم نموذج دارسي لمعادلة الزخم. سمحت لدرجات الحرارة بأن تكون مختلفة في كل من المسامات الكلية والمسامات الجزيئية. كما تمت مناقشة تأثير المعلمات المختلفة على استقراية النظام والتي تضمنت تأثير كل من نسبة التوصيل المعدلة مسامياً وانتقال زخم الطور على بداية الحمل الحراري. علاوة على ذلك، وجد أن حدود الأستقرار غير الخطي لا تتطابق مع حدود عدم الاستقرار الخطي. كما قدمت النتائج العددية في حالة الحدود الحرة.

Introduction

Thermal convection in a bidispersive porous medium is one of much current interest due to its practical applications in various fields, such as in heat pipes technologies, catalytic chemistry, methane recovery from coal deposits, and thermal insulation see e.g., Szczygieł [1], Lin et al. [2], Shi and Durucan [3], Nield and Bejan [4], Straughan [5], and the references

*Email: israa1761986@gmail.com

therein. The funda-mental model for thermal convection in a bidispersive porous medium is due to Nield and Kuznetsov [6-11]. Furthermore important work discussed the problem of thermal convection in a bidispersive porous medium is done by Gentile and Straughan in [12,13]. This has also been considered further using a variety of geometries and incorporating various other effects, for example, anisotropic parameter and double diffusion cf. Straughan [14-17], and Saleh and Haddad [18]. The papers by Franchi et al. [19] present the effect of local thermal non-equilibrium on a bidispersive porous medium. These authors work on development a theory of double porosity material, where the solid skeleton, and the fluid in the micro and macropores may have different temperatures. It is worth to mention that the local thermal non-equilibrium have recently raised much interesting subject. See for example Malashetty et al. [20] investigated the effect of thermal non-equilibrium on the onset of convection when the Lapwood–Brinkman model is included for the momentum equation. The same authors in [21] studied the problem of Onset of convection in an anisotropic porous layer using thermal non-equilibrium. Shivakumara et al. [22] considered the effects of the onset of thermal non-equilibrium convection in a viscoelastic fluid saturate sparsely packed porous layer. Straughan [23] analyzed the linear instability and nonlinear stability boundaries using thermal non-equilibrium model. Malashetty et al. [24] discussed the effect of rotation on thermal convection in a fluid-saturated porous layer with thermal nonequilibrium model. Malashetty and Heera [25] considered the rotation and that the local thermal non-equilibrium effect on double diffusive convection in porous media. Malashetty et al. [26] considered the problem of double diffusive thermal convection in a fluid-saturated porous layer using a thermal non-equilibrium model, while Malashetty et al. [27] investigated thermal non-equilibrium effect on the onset of convection in a couple stress fluid saturated porous medium. Furthermore, Gaikwad et al. [28] explained the combined effect of rotation and local thermal non-equilibrium on the double diffusive convection using linear instability and nonlinear stability methods.

Other aspect of the effect of thermal non-equilibrium on the onset of convection porous layer involving effects like rotation, variable viscosity, density maximum, heterogeneous permeability, and viscous dissipation have been studied by many researchers, e.g., Malashetty and Swamy [29], Shivakumara et al. [30, 31], and Barletta and Celli [32]. Further work using thermal non-equilibrium model has been given by Straughan [5,33], Dayananda and Shivakumara [34], and Santamaria-Holek [35].

In the present paper, we provide an accurate numerical calculation for linear instability and nonlinear stability. In particular, we investigate in details the thermal convection in a bidisperse porous medium where two different temperature fields for the porous solid and for the saturating fluid are assumed in order to model the local thermal non-equilibrium. Moreover, we focus our attention on the effect of different interaction parameters on the critical Rayleigh number. We take this opportunity to point out that the effects of various parameters such as couple stress, uniform magnetic field, permeability of the medium, concentration and the thermo-diffusion, variable viscosity, the velocity and temperature, thermal anisotropy and rotating, are investigated in general by many authors cf. Al-Hhafajy and Abdulhadi [36], Al-Khafajy and Labban [37], Kareem and Abdulhadi [38], Khudair and Al-Khafajy [39], and Haddad [40,41].

The paper is organized as follows: In section 2 the basic equations and the nondimensionalized perturbation equations are presented. The linear stability and the nonlinear stability analysis are the subject of sections 3 and 4. In section 5 the numerical results are reported.

Governing Equations

The equations for a bidispersive local thermal non-equilibrium flow in a Darcy porous material are derived in Franchi et al. [19], with U_i^f and U_i^p being the pore-averaged

velocities in the macro and micropores, p^f and p^p are the pressures in the macro and micropores, μ is the dynamic viscosity, g_i is the gravity vector, ρ is the density, and k_f k_p are the permeability in the macro and micropores, and ζ is an interaction coefficient. We suppose that the saturated porous medium is occupying the three dimensional layer $\{(x,y)\in R^2\}\times\{0<z<d\}$ with the temperatures $T^s=T^f=T^p=T_L$, at $z=0$, and $T^s=T^f=T^p=T_U$, at $z=d$, where T_L, T_U are constants with $T_L>T_U$. The governing equations consist of the momentum and Continuity equations and adopting the Boussinesq approximation in the macro and micropores of Darcy type may be found in Nield and Kuznetsov [8], Straughan [5], and Franchi et al. [19],

$$\begin{aligned}
&\frac{-\mu}{k_f}U_i^f-\zeta(U_i^f-U_i^p)-p_{,i}^f-\frac{g_i\rho_o\alpha\varphi}{D}T^f-\frac{g_i\rho_o\alpha(1-\varphi)\varepsilon}{D}T^p=0,\\
&U_{i,i}^f=0,\\
&\frac{-\mu}{k_p}U_i^p-\zeta(U_i^p-U_i^f)-p_{,i}^p-\frac{g_i\rho_o\alpha\varphi}{D}T^f-\frac{g_i\rho_o\alpha(1-\varphi)\varepsilon}{D}T^p=0,\\
&U_{i,i}^p=0,
\end{aligned}\tag{1}$$

where $D=\varphi+(1-\varphi)\varepsilon$, T^f, T^p, and T^s, respectively, are reference values of temperature in the macro pore, micropores, and solid skeleton. ϕ is the macroporosity, ε is the microporosity. Standard indicial notation is employed in (1) and throughout. We let $U_i^f=\varphi V_i^f$ and $U_i^p=(1-\varphi)\varepsilon V_i^p$ to be the fluid velocities in the macro and micropores , V_i^f and V_i^p are the pore average velocities in the macro and micropores. The balance of energy equations for the temperature is established as in Franchi et al. [19], and can be written as

$$\begin{aligned}
&\varepsilon_1(\rho c)_s T_{,t}^s=\varepsilon_1 k_s\Delta T^s+s_1(T^f-T^s)+s_2(T^p-T^s),\\
&\varphi(\rho c)_f T_{,t}^f+\varphi(\rho c)_f V_i^f T_{,i}^f=\varphi k_f\Delta T^f+h(T^p-T^f)+s_1(T^s-T^f),\\
&\varepsilon_2(\rho c)_p T_{,t}^p+\varepsilon_2(\rho c)_p V_i^p T_{,i}^p=\varepsilon_2 k_p\Delta T^p+h(T^f-T^p)+s_1(T^s-T^p),
\end{aligned}\tag{2}$$

where $\varepsilon_1=(1-\varepsilon)(1-\varphi)$, $\varepsilon_2=(1-\varphi)\varepsilon$. Here $(\rho c)_s$, $(\rho c)_f$, $(\rho c)_p$ are the products of the density and the specific heat at constant pressure in the solid in the fluid in the macro pores, and in the fluid in the micropores, respectively. The terms k_s, k_f, and k_p are thermal conductivities in the solid, and in the fluid in the macro and micropores, respectively. We denote by s, f, and p the solid, the macro pores, and the micropores the terms h, s_1, and s_2 are interaction coefficients, and we have here assumed that the interactions are linear in the temperature differences.

We suppose that the fluid saturated bidispersive porous medium satisfies equation (1) and equation (2). The velocity boundary conditions are $U_i^f n_i=0, U_i^p n_i=0$ at $z=0,d$. The steady solution in whose stability we are interested has form

$\bar{U}_i^f\equiv 0$, $\bar{U}_i^p\equiv 0$, $\bar{T}^s=\bar{T}^f=\bar{T}^p=-\beta z+T_L=0$,

where

$\beta=\frac{T_L-T_U}{d}$.

To investigate the stability of the steady solution, we introduce perturbation $\left(u_i^f, u_i^p, \pi^f, \pi^p, \theta^f, \theta^p\right)$ in such a way that

$U_i^f = \bar{U}_i^f + u_i^f$, $U_i^p = \bar{U}_i^p + u_i^p$, $p^f = \bar{p}^f + \pi^f$, $p^p = \bar{p}^p + \pi^p$,

$T^s = \bar{T}^s + \theta^s$, $T^f = \bar{T}^f + \theta^f$, $T^p = \bar{T}^p + \theta^p$.

The nonlinear perturbation equations arising from equation (1) and equation (2) are

$$\frac{-\mu}{k_f}u_i^f - \zeta(u_i^f - u_i^p) - \pi_{,i}^f - \frac{g\,k_i\rho_0\alpha\varphi}{D}\theta^f - \frac{g\,k_i\rho_0\alpha(1-\varphi)\varepsilon}{D}\theta^p = 0,$$

$$u_{i,i}^f = 0,$$

$$\frac{-\mu}{k_p}u_i^f - \zeta(u_i^p - u_i^f) - \pi_{,i}^p - \frac{g\,k_i\rho_0\alpha\varphi}{D}\theta^f - \frac{g\,k_i\rho_0\alpha(1-\varphi)\varepsilon}{D}\theta^p = 0,$$

$$u_{i,i}^p = 0, \tag{3}$$

$$\varepsilon_1(\rho c)_s\theta_{,t}^s = \varepsilon_1 k_s\Delta\theta^s + s_1(\theta^f - \theta^s) + s_2(\theta^p - \theta^s),$$

$$\varphi(\rho c)_f\theta_{,t}^f + (\rho c)_f u_i^f\theta_{,i}^f - (\rho c)_f\beta w^f = \varphi k_f\Delta\theta^f + h(\theta^p - \theta^f) + s_1(\theta^s - \theta^f),$$

$$\varepsilon_2(\rho c)_p\theta_{,t}^p + (\rho c)_p u_i^p\theta_{,i}^p - (\rho c)_p\beta w^p = \varepsilon_2 k_p\Delta\theta^p + h(\theta^f - \theta^p) + s_2(\theta^s - \theta^p),$$

where $w^f = u_3^f$ and $w^p = u_3^p$, while $k_i = (0,0,1)$. We then introduce the nondimensionalizations scale with length scale d, time scale τ, pressure p, velocity U, and temperature scale

$$\tau = \frac{d^2(\rho c)_f}{k_f},\ p = d\zeta U,\ U = \frac{k_f}{(\rho c)_f d},\ T^{\#} = u\sqrt{\frac{(\rho c)_f d^2\beta\zeta}{g\rho_o\alpha\varphi k_f}},$$

and the Rayleigh number $R_a = R^2$ is given by

$$R^2 = \frac{(\rho c)_f d^2\beta g\rho_o\alpha}{\zeta\varphi k_f}.$$

Other nondimensional variables are required and these are given by

$$\mu_1 = \frac{\mu}{k_f\zeta},\quad \mu_2 = \frac{\mu}{k_p\zeta},\quad L_s = \frac{(\rho c)_s}{(\rho c)_f},\quad \xi_s = L_s\frac{\varepsilon_1}{\varphi},\quad S_1 = \frac{s_1 d^2}{\varphi k_f},\quad S_2 = \frac{s_2 d^2}{\varphi k_f},$$

$$H = \frac{hd^2}{\varphi k_f},\quad \Gamma_s = \frac{\varepsilon_1 k_s}{\varphi k_f}\quad \Gamma_p = \frac{\varepsilon_2 k_p}{\varphi k_f},\quad L_P = \frac{(\rho c)_p}{(\rho c)_f},\quad \xi_p = L_P\frac{\varepsilon_2}{\varphi}.$$

The nondimensional equations which is Achieved from equation (3) are

$$\mu_1 u_i^f + (u_i^f - u_i^p) = -\pi_{,i}^f + R\frac{\varphi k_i}{D}\theta^f + R\frac{(1-\varphi)\varepsilon k_i}{D}\theta^P,\qquad u_{i,i}^f = 0,$$

$$\mu_2 u_i^p + (u_i^p - u_i^f) = -\pi_i^p + R\frac{\varphi k_i}{D}\theta^f + R\frac{(1-\varphi)\varepsilon k_i}{D}\theta^P,\qquad u_{i,i}^p = 0,$$

$$\xi_s\theta_{,t}^s = \Gamma_s\Delta\theta^s + S_1(\theta^f - \theta^s) + S_2(\theta^p - \theta^s), \tag{4}$$

$$\theta_{,t}^p + \frac{1}{\varphi}u_i^f\theta_{,i}^f = Rw^f + \Delta\theta^f + H(\theta^p - \theta^f) + S_1(\theta^s - \theta^f),$$

$$\xi_p\theta_{,t}^p + \frac{L_p}{\varphi}u_i^p\theta_{,i}^p = RL_p w^p + L_p\Delta\theta^p + H(\theta^f - \theta^p) + S_2(\theta^s - \theta^p).$$

Equation (4) hold on $\{(x,y)\grave{o}R^2\}'\ \{0< z< d\}$ and the boundary conditions

$$w^f = u_3^f = 0,\ w^p = u_3^p = 0,\ \theta^f = 0,\ \theta^p = 0,\ \theta^s = 0,\ \text{at } z = 0,1, \tag{5}$$

with $u_i^f = \left(u^f, v^f, w^f\right)$ and $u_i^p = \left(u^p, v^p, w^p\right)$ are satisfying on plane tiling periodicity in (x,y)

.**Solution of Linear Stability Equations**

In this section, we seek to find the critical Rayleigh number of linear theory, we first linearize equation (3) then we write the variables $u_i^f, u_i^p, \pi^f, \pi^p, \theta^f, \theta^p,$ and θ^s by explicitly separating the time dependent parts and we follow the work of Chandrasekhar [42] by imposing a temporal growth rate like $e^{\sigma t}$ for solutions of the form

$$u_i^f = u_i^f(x)e^{\sigma t},\ \ u_i^p = u_i^p(x)e^{\sigma t},\ \ \pi^f = \pi^f(x)e^{\sigma t},\ \ \pi^p = \pi^p(x)e^{\sigma t},$$

$$\theta^f = \theta^f(x)e^{\sigma t},\ \ \theta^p = \theta^p(x)e^{\sigma t},\ \ \theta^s = \theta^s(x)e^{\sigma t}.$$

Then π^f and π^p are eliminated by taking curl of equation $(4)_1$ and equation $(4)_2$, and then analysis the linear system. The linear system arising from equation (4) is

$$\begin{aligned}
&\mu_1\Delta w^f + (\Delta w^f - \Delta w^p) - R\frac{\varphi}{D}\Delta^*\theta^f - R\frac{(1-\varphi)\varepsilon}{D}\Delta^*\theta^p = 0,\\
&\mu_2\Delta w^p + (\Delta w^p - \Delta w^f) - R\frac{\varphi}{D}\Delta^*\theta^f - R\frac{(1-\varphi)\varepsilon}{D}\Delta^*\theta^p = 0,\\
&\sigma\xi_s\theta_{,t}^s = \Gamma_s\Delta\theta^s + S_1(\theta^f - \theta^s) + S_2(\theta^p - \theta^s),\\
&\sigma\theta_{,t}^f = Rw^f + \Delta\theta^f + H(\theta^p - \theta^f) + S_1(\theta^s - \theta^f),\\
&\sigma\xi_p\theta_{,t}^p = RL_p w^p + \Gamma_p\Delta\theta^p + H(\theta^f - \theta^p) + S_2(\theta^s - \theta^p),
\end{aligned} \tag{6}$$

where $\Delta^* = \partial^2/\partial x^2 + \partial^2/\partial y^2$ is the horizontal Laplacian. This is an eigenvalue problem for σ to be solved subject to the boundary conditions in equation (5).

To analyze (6) and (5), assume normal mode with the representations for w^f, w^p, θ^f, θ^p, and θ^s in the form of

$$\theta^f = \Theta^f(z)f(x,y),\quad \theta^p = \Theta^p(z)f(x,y),\quad \theta^s = \Theta^s(z)f(x,y),$$

$$w^f = W^f(z)f(x,y),\quad w^p = W^p(z)f(x,y),$$

where f is the horizontal plan form, which satisfies $\Delta^* f = -a^2 f$, a is a wave number. Then, we allow W^f, W^p, Θ^f, Θ^p, and Θ^s to be composed of $\sin n\pi z$, for $n \in N$ which satisfies the boundary conditions (5). The system (6) can be written in the matrix form

$$\begin{bmatrix} -(\mu_1+1)\Lambda & \Lambda & R\frac{\varphi}{D}a^2 & R\frac{(1-\varphi)\varepsilon}{D}a^2 & 0 \\ \Lambda & -(\mu_2+1)\Lambda & R\frac{\varphi}{D}a^2 & R\frac{(1-\varphi)\varepsilon}{D}a^2 & 0 \\ 0 & 0 & -S_1 & -S_2 & \xi_S\sigma+\Gamma_S\Lambda+S_1+S_2 \\ -R & 0 & \sigma+\Lambda+H+S_1 & -H & -S_1 \\ 0 & -L_pR & -H & \xi_p\sigma+\Gamma_p\Lambda+H+S_2 & -S_2 \end{bmatrix} \begin{bmatrix} W^f \\ W^p \\ \Theta^f \\ \Theta^p \\ \Theta^s \end{bmatrix} = \begin{bmatrix} 0 \\ 0 \\ 0 \\ 0 \\ 0 \end{bmatrix}, \quad (7)$$

where $\Lambda = n^2\pi^2 + a^2$. Then, one may consider the following two cases.

3.1 Stationary Convection ($\sigma = 0$).

Substituting ($\sigma = 0$) in (6). The stationary convection boundary is given by

$$R^2 = \frac{D\Lambda[k_0A_1 + k_0A_2]}{a^2[\varphi(k_2B_3 - k_1B_1) + (1-\varphi)\varepsilon(k_1B_2 - k_2B_4)]}. \quad (8)$$

With the coefficients $k_0, k_1, k_2, A_1, A_2, B_1, B_2, B_3$, and B_4 are given by

$k_0 = 1-(\mu_1+1)(\mu_2+1),$

$k_1 = 1+(\mu_1+1),$

$k_2 = 1+(\mu_2+1),$

$A_1 = 2S_1S_2H + S_2^2(\Lambda+H+S_1) + H^2(\Gamma_s\Lambda+S_1+S_2),$

$A_2 = (\Gamma_p\Lambda+H+S_2)(S_1^2 - (\Lambda+H+S_1)(\Gamma_s\Lambda+S_1+S_2)),$

$B_1 = S_1S_2L_p + L_pH(\Gamma_s\Lambda+S_1+S_2),$

$B_2 = S_1^2L_p - L_p(\Lambda+H+S_1)(\Gamma_s\Lambda+S_1+S_2),$

$B_3 = (S_2^2 - (\Gamma_s\Lambda+S_1+S_2)(\Gamma_p\Lambda+H+S_2),$

$B_4 = S_1S_2 + H(\Gamma_s\Lambda+S_1+S_2).$

Then one can show $\partial R^2/\partial n^2 > 0$. Therefore, we select $n = 1$ to obtain the lowest instability boundary.

3.2 Oscillatory Convection ($\sigma = i\sigma_I$), where $\sigma_I \in \mathrm{R}$.

To study oscillatory convection put $\sigma = i\sigma_I$ in equation (6), where $\sigma_I \in \mathrm{R}$. We solve the determinant equation, then we have

$$R^2 = \frac{D\Lambda[k_0(h_1+h_2+h_3)]}{-a^2[k_1L_p\xi_s(1-\varphi)\varepsilon + k_2\varphi\xi_s\xi_p]}. \quad (9)$$

Here, the coefficients h_1, h_2 and h_3 are defined by

$h_1 = \xi_s(\Gamma_p\Lambda+H+S_2),$

$h_2 = \xi_p(\Gamma_s\Lambda+S_1+S_2),$

$h_3 = \xi_s\xi_p(\Lambda+H+S_1).$

Numerical techniques are used to find the stationary convection threshold Ra_{sta} and oscillatory convection threshold Ra_{ost}, respectively. We minimize R^2 in (8) and (9) over a^2, as will be presented in the numerical results section.

Nonlinear Stability Analysis

Let $_v$ be a period cell for the solution to (4) and (5), and let $\|\cdot\|$, $(\cdot,\cdot)$ be the norm and inner product on $L^2(V)$. We commence by multiplying $(4)_1$ by u_i^f, $(4)_2$ by u_i^p, We also multiply $(4)_3$ by θ^s, $(4)_4$ by θ^f, $(4)_5$ by θ^p and integrate each over V. Thus, we derive the following equations:

$$\mu_1\|\mathbf{u}^f\|^2+\|\mathbf{u}^f\|^2-\left(u_i^p,u_i^f\right)-R\frac{\varphi}{D}\left(\theta^f,w^f\right)-R\frac{(1-\varphi)\varepsilon}{D}\left(\theta^p,w^f\right)=0$$

$$\mu_2\|\mathbf{u}^p\|^2+\|\mathbf{u}^p\|^2-\left(u_i^f,u_i^p\right)-R\frac{\varphi}{D}\left(\theta^f,w^p\right)-R\frac{(1-\varphi)\varepsilon}{D}\left(\theta^p,w^p\right)=0$$

$$\frac{1}{2}\frac{d}{dt}\xi_s\|\theta^s\|^2=-\Gamma_s\|\nabla\theta^s\|^2+S_1\left(\theta^f,\theta^s\right)-S_1\|\theta^s\|^2+S_2\left(\theta^p,\theta^s\right)-S_2\|\theta^s\|^2 \quad . \quad (10)$$

$$\frac{1}{2}\frac{d}{dt}\|\theta^f\|^2=-\|\nabla\theta^f\|^2+R\left(w^f,\theta^f\right)+H\left(\theta^p,\theta^f\right)-H\|\theta^f\|^2+S_1\left(\theta^s,\theta^f\right)-S_1\|\theta^f\|^2$$

$$\frac{1}{2}\frac{d}{dt}\xi_p\|\theta^p\|^2=-\Gamma_p\|\nabla\theta^p\|^2+RL_P\left(w^p,\theta^p\right)+H\left(\theta^f,\theta^p\right)-H\|\theta^p\|^2+S_2\left(\theta^s,\theta^p\right)-S_2\|\theta^p\|^2.$$

To determine the parameter $\lambda>0$ we now form $\lambda(10)_3+\lambda(10)_4+\lambda(10)_5$, to obtain an energy identity of form

$$\frac{dE}{dt}=RI-\mathsf{D} \quad (11)$$

where

$$E(t)=\frac{\lambda}{2}\left[\xi_s\|\theta^s\|^2+\|\theta^f\|^2+\xi_p\|\theta^p\|^2\right],$$

$$I=\left(\sqrt{\lambda}+\frac{\varphi}{D\sqrt{\lambda}}\right)\left(w^f,\theta^f\right)+\left(\sqrt{\lambda}L_p+\frac{(1-\varphi)\varepsilon}{D\sqrt{\lambda}}\right)\left(w^p,\theta^p\right)+\frac{\varphi}{D\sqrt{\lambda}}\left(\theta^f,w^p\right)+\frac{(1-\varphi)\varepsilon}{D\sqrt{\lambda}}\left(\theta^p,w^f\right),$$

$$\mathsf{D}=\Gamma_s\|\nabla\theta^s\|^2+\|\nabla\theta^f\|^2+\Gamma_p\|\nabla\theta^p\|^2+\mu_1\|\mathbf{u}^f\|^2+\mu_2\|\mathbf{u}^p\|^2+\|\mathbf{u}^f-\mathbf{u}^p\|^2+S_1\|\theta^f-\theta^s\|^2$$
$$+S_2\|\theta^p-\theta^s\|^2+H\|\theta^p-\theta^f\|^2 \quad .$$

Equation (11) is the same as the expression was report by Straughan [5].

Now put

$$\frac{1}{R_E}=\max_{\aleph}\frac{I}{\mathsf{D}}, \quad (12)$$

where $\aleph$ is the space of admissible functions which are given by

$$\left\{\begin{array}{l}\aleph = u_i^f, u_i^p, \theta^s, \theta^f, \theta^p \,\middle|\, u_i^f, u_i^p \in L^2(V), \theta^s, \theta^f, \theta^p \in \aleph^1(V), \\ \nabla u_i^f = 0, \nabla u_i^p = 0, u_i^f, u_i^p, \theta^s, \theta^f, \theta^p, \text{ are periodic in } x, y, \\ \text{and } w_i^f = w_i^p = \theta^s = \theta^f = \theta^p = 0, \text{ on } z = 0,1.\end{array}\right\}.$$

Then from (12), we deduce

$$\frac{dE}{dt} \le -\mathsf{D}(1-\frac{R}{R_E}).$$

and then, from the Poincaré's inequality on D, we have $\frac{dE}{dt} \le -c'\pi^2 \|\theta\|^2$,

which integrates to

$$E(t) \le E(0)e^{-c't}.$$

Thus, $E(t)$ tends to 0 as $t \to \infty$ at least exponentially. Therefore, $\|\theta^f\| \to 0$, $\|\theta^p\| \to 0$ and $\|\theta^s\| \to 0$ at least exponential.

To obtain the decay of $\|\mathbf{u}^f\|$ and $\|\mathbf{u}^p\|$, we have to employ the arithmetic geometric mean inequality in $(10)_1$ and $(10)_2$

$$(1+\mu_1)\|u^f\|^2 \le \frac{R\varphi}{2D\alpha_1}\|\theta^f\|^2 + \frac{R\varphi\alpha_1}{2D}\|w^f\|^2 + \frac{R(1-\varphi)\varepsilon\beta_1}{2D}\|\theta^f\|^2,$$

$$(1+\mu_2)\|u^p\|^2 \le \frac{R\varphi}{2D\alpha_2}\|\theta^p\|^2 + \frac{R\varphi\alpha_2}{2D}\|w^p\|^2 + \frac{R(1-\varphi)\varepsilon\beta_2}{2D}\|\theta^p\|^2 + \frac{R(1-\varphi)\varepsilon}{2D\beta_2}\|w^p\|^2.$$

$$\frac{1}{2}\left\{(1+\mu_1)\|u^f\|^2 + (1+\mu_2)\|u^p\|^2\right\} \le \left\{\frac{1}{(1+\mu_1)} + \frac{1}{(1+\mu_2)}\right\}\frac{R^2}{D^2}\left\{\varphi^2\|\theta^f\|^2 + (1-\varphi)^2\varepsilon^2\|\theta^p\|^2\right\}$$

We let

$$\alpha_1 = \frac{(1+\mu_1)D}{2R\varphi}, \quad \alpha_2 = \frac{(1+\mu_2)D}{2R\varphi}, \quad \beta_1 = \frac{2R(1-\varphi)\varepsilon}{D(1+\mu_1)}, \quad \beta_2 = \frac{2R(1-\varphi)\varepsilon}{D(1+\mu_2)},$$

$$\frac{1}{2}\left\{(1+\mu_1)\|u^f\|^2 + (1+\mu_2)\|u^p\|^2\right\} \le \left\{\frac{1}{(1+\mu_1)} + \frac{1}{(1+\mu_2)}\right\}\frac{R^2}{D^2}\left\{\varphi^2\|\theta^f\|^2 + (1-\varphi)^2\varepsilon^2\|\theta^p\|^2\right\},$$

where the decay of $\mathbf{u}^f$ and $\mathbf{u}^p$ follow. We now turn our attention to the maximization problem (12) with $R_E > 1$.

In order to determine R_E, we have to derive the Euler–Lagrange equations and to maximize in the coupling parameter λ. The Euler–Lagrange equations arising from equation (12) are determined from

$$R_E\,\delta I - \delta\mathsf{D} = 0.$$

Let us define u_i^f, u_i^p, θ^f, θ^p, and θ^s in terms of arbitrary $C^2(0,1)$ functions h_i^f, h_i^p, η^f, η^p, and η^s with $h_i^f(0) = h_i^f(1) = h_i^p(0) = h_i^p(1) = 0$ and

$$\eta^f(0) = \eta^f(1) = \eta^p(0) = \eta^p(1) = \eta^s(0) = \eta^s(1) = 0.$$

Hence we have that

$$\delta \mathsf{D} = \int_V [\Gamma_s \nabla \left(\theta^s + \varepsilon\eta^s\right)^2 + \nabla \left(\theta^f + \varepsilon\eta^f\right)^2 + \Gamma_p \nabla \left(\theta^p + \varepsilon\eta^p\right)^2 + \mu_1 \left(u_i^f + \varepsilon h_i^f\right)^2 + \mu_2 \left(u_i^p + \varepsilon h_i^p\right)^2$$
$$+ \left(u_i^f + \varepsilon h_i^f - \left(u_i^p + \varepsilon h_i^p\right)\right)^2 + S_1 \left(\theta^f + \varepsilon\eta^f - \left(\theta^s + \varepsilon\eta^s\right)\right)^2 + S_2 \left(\theta^p + \varepsilon\eta^p - \left(\theta^s + \varepsilon\eta^s\right)\right)^2$$
$$+ H \left(\theta^p + \varepsilon\eta^p - \left(\theta^f + \varepsilon\eta^f\right)\right)^2] \mathrm{dV}\big|_{\varepsilon=0},$$
$$\delta \mathsf{D} = \int_V [2\Gamma_s \nabla \left(\theta^s + \varepsilon\eta^s\right) \nabla \eta^s + 2\nabla \left(\theta^f + \varepsilon\eta^f\right) \nabla \eta^f + 2\Gamma_p \nabla \left(\theta^p + \varepsilon\eta^p\right) \nabla \eta^p + 2\mu_1 \left(u_i^f + \varepsilon h_i^f\right) h_i^f$$
$$+ 2\mu_2 \left(u_i^p + \varepsilon h_i^p\right) h_i^p + 2\left(u_i^f + \varepsilon h_i^f - \left(u_i^p + \varepsilon h_i^p\right)\right)\left(h_i^f - h_i^p\right) + 2S_1 \left(\theta^f + \varepsilon\eta^f - \left(\theta^s + \varepsilon\eta^s\right)\right)\left(\eta^f - \eta^s\right)$$
$$+ 2S_2 \left(\theta^p + \varepsilon\eta^p - \left(\theta^s + \varepsilon\eta^s\right)\right) + 2H \left(\theta^p + \varepsilon\eta^p - \left(\theta^f + \varepsilon\eta^f\right)\right)\left(\eta^p - \eta^f\right)] \mathrm{dV}\big|_{\varepsilon=0},$$

and

$$\delta I = \frac{d}{d\varepsilon} \int_V [\left(\sqrt{\lambda} + \frac{\varphi}{D\sqrt{\lambda}}\right)\left(w^f + \varepsilon h_3^f\right)\left(\theta^f + \varepsilon\eta^f\right) + \left(\sqrt{\lambda} L_p + \frac{(1-\varphi)\varepsilon}{D\sqrt{\lambda}}\right)\left(w^p + \varepsilon h_3^p\right)\left(\theta^p + \varepsilon\eta^p\right)$$
$$+ \frac{\varphi}{D\sqrt{\lambda}}\left(\theta^f + \varepsilon\eta^f\right)\left(w^p + \varepsilon h_3^p\right) + \frac{(1-\varphi)\varepsilon}{D\sqrt{\lambda}}\left(\theta^p + \varepsilon\eta^p\right)\left(w^f + \varepsilon h_3^f\right) - (u_{i,i}^f + \varepsilon h_{i,i}^f)\pi^f(\mathrm{x}) - (u_{i,i}^p + \varepsilon h_{i,i}^p)\pi^p(\mathrm{x})] dV \Big|_{\varepsilon=0},$$

$$\delta I = \int_V [\left(\sqrt{\lambda} + \frac{\varphi}{D\sqrt{\lambda}}\right)[\left(w^f + \varepsilon h_3^f\right)\eta^f + \left(\theta^f + \varepsilon\eta^f\right)h_3^f] + \left(\sqrt{\lambda} L_p + \frac{(1-\varphi)\varepsilon}{D\sqrt{\lambda}}\right)[\left(w^p + \varepsilon h_3^p\right)\eta^p + \left(\theta^p + \varepsilon\eta^p\right)h_3^p]$$
$$+ \frac{\varphi}{D\sqrt{\lambda}}[\left(\theta^f + \varepsilon\eta^f\right)h_3^p + \left(w^p + \varepsilon h_3^p\right)\eta^f] + \frac{(1-\varphi)\varepsilon}{D\sqrt{\lambda}}[\left(\theta^p + \varepsilon\eta^p\right)h_3^f + \left(w^f + \varepsilon h_3^f\right)\eta^p - h_{i,i}^f \pi^f(\mathrm{x}) - h_{i,i}^p \pi^p(\mathrm{x})] dV \Big|_{\varepsilon=0},$$

we have included the constraint $u_{i,i}^f$ and $u_{i,i}^p$ by using a Lagrange multiplier $\pi(\mathrm{x})$, and ε is a positive constant. Furthermore, after some integrations by parts and using the boundary conditions, we find that

$$\delta \mathsf{D} = \int_V 2[\Gamma_s \nabla\theta^s \nabla\eta^s + \nabla\theta^f \nabla\eta^f + \Gamma_p \nabla\theta^p \nabla\eta^p + \mu_1 u_i^f h_i^f + \mu_2 u_i^p h_i^p + (u_i^f - u_i^p)(h_i^f - h_i^p) + S_1(\theta^f - \theta^s)(\eta^f - \eta^s)$$
$$+ S_2(\theta^p - \theta^s)(\eta^p - \eta^s) + H(\theta^p - \theta^f)(\eta^p - \eta^f)] dV,$$

$$\delta I = \int_V [\left(\sqrt{\lambda} + \frac{\varphi}{D\sqrt{\lambda}}\right)\left(w^f \eta^f + \theta^f h_3^f\right) + \left(\sqrt{\lambda} L_p + \frac{(1-\varphi)\varepsilon}{D\sqrt{\lambda}}\right)\left(w^p \eta^p + \theta^p h_3^p\right) + \frac{\varphi}{D\sqrt{\lambda}}\left(\theta^f h_3^p + w^p \eta^f\right)$$
$$+ \frac{(1-\varphi)\varepsilon}{D\sqrt{\lambda}}\left(\theta^p h_3^f + w^f \eta^p\right) - h_i^f \pi_{,i}^f - h_{i,i}^p \pi_{,i}^p] dV.$$

Then the Euler–Lagrange equations for the maximum problem (12) are

$$\mu_1 u_i^f + (u_i^f - u_i^p) - R_E(\frac{\sqrt{\lambda}}{2} + \frac{\varphi}{2D\sqrt{\lambda}})\theta^f k_i - R_E \frac{(1-\varphi)\varepsilon}{2D\sqrt{\lambda}})\theta^p k_i = \pi_{,i}^f,$$

$$\mu_2 u_i^p + (u_i^p - u_i^f) - R_E \frac{\varphi}{2D\sqrt{\lambda}}\theta^f k_i - R_E(L_p \frac{\sqrt{\lambda}}{2} + \frac{(1-\varphi)\varepsilon}{2D\sqrt{\lambda}})\theta^p k_i = \pi_{,i}^f,$$

$$\Gamma_s \Delta\theta^s + S_1(\theta^f - \theta^s) + S_2(\theta^p - \theta^s) = 0, \tag{14}$$

$$R_E(\frac{\sqrt{\lambda}}{2} + \frac{\varphi}{2D\sqrt{\lambda}})w^f + R_E \frac{\varphi}{2D\sqrt{\lambda}} w^p + \Delta\theta^f + S_1(\theta^s - \theta^f) + H(\theta^p - \theta^f) = 0,$$

$$R_E \frac{(1-\varphi)\varepsilon}{2D\sqrt{\lambda}})w^f + R_E(L_p \frac{\sqrt{\lambda}}{2} + \frac{(1-\varphi)\varepsilon}{2D\sqrt{\lambda}})w^p + \Gamma_p \Delta\theta^p + S_2(\theta^s - \theta^p) + H(\theta^f - \theta^p) = 0,$$

where π^f and π^p are Lagrange multipliers. Further progress is made by taking curl of equation $(14)_1$ and equation $(14)_2$, we obtain

$$\mu_1 \Delta w^f + (\Delta w^f - \Delta w^p) - R_E(\frac{\sqrt{\lambda}}{2} + \frac{\varphi}{2D\sqrt{\lambda}})\Delta^* \theta^f - R_E \frac{(1-\varphi)\varepsilon}{2D\sqrt{\lambda}})\Delta^* \theta^p = 0,$$

$$\mu_2 \Delta w^p + (\Delta w^p - \Delta w^f) - R_E \frac{\varphi}{2D\sqrt{\lambda}} \Delta^* \theta^f - R_E(L_p \frac{\sqrt{\lambda}}{2} + \frac{(1-\varphi)\varepsilon}{2D\sqrt{\lambda}})\Delta^* \theta^p = 0,$$

$$\Gamma_s \Delta\theta^s + S_1(\theta^f - \theta^s) + S_2(\theta^p - \theta^s) = 0,$$

$$R_E(\frac{\sqrt{\lambda}}{2} + \frac{\varphi}{2D\sqrt{\lambda}})w^f + R_E \frac{\varphi}{2D\sqrt{\lambda}} w^p + \Delta\theta^f + S_1(\theta^s - \theta^f) + H(\theta^p - \theta^f) = 0,$$

$$R_E \frac{(1-\varphi)\varepsilon}{2D\sqrt{\lambda}})w^f + R_E(L_p \frac{\sqrt{\lambda}}{2} + \frac{(1-\varphi)\varepsilon}{2D\sqrt{\lambda}})w^p + \Gamma_p \Delta\theta^p + S_2(\theta^s - \theta^p) + H(\theta^f - \theta^p) = 0.$$

(15)

We again use a normal mode representation as for the linear stability analysis in section 3. These results are to solve the determinant equation

$$\begin{bmatrix} -(\mu_1+1)\Lambda & \Lambda & R_E(\frac{\sqrt{\lambda}}{2}+c)a^2 & R_E b a^2 & 0 \\ \Lambda & -(\mu_2+1)\Lambda & R_E c a^2 & R_E(L_p\frac{\sqrt{\lambda}}{2}+b)a^2 & 0 \\ 0 & 0 & S_1 & S_2 & -(\Gamma_s\Lambda+S_1+S_2) \\ R_E(\frac{\sqrt{\lambda}}{2}+c) & R_E c & -(\Lambda+S_1+H) & H & S_1 \\ R_E b & R_E(L_p\frac{\sqrt{\lambda}}{2}+b) & H & -(\Gamma_p\Lambda+S_2+H) & S_2 \end{bmatrix} \begin{bmatrix} W^f \\ W^p \\ \Theta^f \\ \Theta^p \\ \Theta^s \end{bmatrix} = \begin{bmatrix} 0 \\ 0 \\ 0 \\ 0 \\ 0 \end{bmatrix}, \tag{16}$$

where $c = \dfrac{\varphi}{2D\sqrt{\lambda}}$ and $b = \dfrac{(1-\varphi)\varepsilon}{2D\sqrt{\lambda}}$. The corresponding boundary conditions are

$W^f = 0,\ W^p = 0,\ \Theta^f = 0,\ \Theta^p = 0,\ \Theta^s = 0,$ at $z = 0,1.$

We follow the same procedure to that used in the linear instability. set the determinant of the matrix to zero, we arrive at the equation in R_E

$$AR_E^4 + BR_E^2 + C = 0, \tag{17}$$

with coefficients

$A = -a^4\gamma_1,\quad B = a^2\Lambda(\Omega_1 - \Omega_2 + \Omega_3),\quad C = -\Lambda^2 k_0(\gamma_2 + \gamma_3) = 0,$

Where

$$\Omega_1 = (\Gamma_s\Lambda + S_1 + S_2)\,H[2(\mu_1+1)(L_p\frac{\sqrt{\lambda}}{2} + b)\,c + 2(\mu_2+1)(\frac{\sqrt{\lambda}}{2} + c)\,b]$$
$$+ (\Gamma_s\Lambda + S_1 + S_2)(\Gamma_p\Lambda + S_2 + H)[(\mu_1+1)\,c^2 + (\mu_2+1)(\frac{\sqrt{\lambda}}{2} + c)^2]$$
$$+ (\Gamma_s\Lambda + S_1 + S_2)(\Lambda + S_1 + H)[(\mu_1+1)(L_p\frac{\sqrt{\lambda}}{2} + b)^2 + (\mu_2+1)\,b^2],$$

$$\Omega_2 = (\mu_1+1)\left(S_1\left(L_p\frac{\sqrt{\lambda}}{2} + b\right) + S_2 c\right)^2 + (\mu_1+1)\left(S_1 b - S_2\left(\frac{\sqrt{\lambda}}{2} + c\right)\right)^2,$$

$$\Omega_3 = ((\frac{\sqrt{\lambda}}{2} + c)(L_p\frac{\sqrt{\lambda}}{2} + b) + bc)(2H(\Gamma_s\Lambda + S_1 + S_2) + 2S_1S_2)$$
$$+ (L_p\frac{\sqrt{\lambda}}{2} + b)b(2(\Gamma_s\Lambda + S_1 + S_2)(\Lambda + S_1 + H) - 2S_1^2)$$
$$+ (\frac{\sqrt{\lambda}}{2} + c)c(2(\Gamma_s\Lambda + S_1 + S_2)(\Gamma_p\Lambda + S_2 + H) - 2S_2^2),$$

and

$$\gamma_1 = (\Gamma_s\Lambda + S_1 + S_2)((\frac{\sqrt{\lambda}}{2} + c)(L_p\frac{\sqrt{\lambda}}{2} + b) - bc)^2,$$
$$\gamma_2 = (\Gamma_s\Lambda + S_1 + S_2)(H^2 - (\Lambda + S_1 + H)(\Gamma_p\Lambda + S_2 + H)),$$
$$\gamma_3 = 2S_1S_2(2H + S_1(\Gamma_p\Lambda + S_2 + H) + S_2(\Lambda + S_1 + H).$$

The energy Rayleigh number R_E^2 is then given by

$$R_E^2 = \frac{\Lambda[(\Omega_1 - \Omega_2 + \Omega_3) \pm \sqrt{(\Omega_1 - \Omega_2 + \Omega_3)^2 - 4\gamma_1 k_0(\gamma_2 + \gamma_3)}]}{2a^2\gamma_1}. \tag{18}$$

We require to find the critical nonlinear Rayleigh number Ra_E, such that

$$Ra_E = \max_{\lambda}\min_{a^2} R_E^2\left(a^2, \lambda\right).$$

Numerical results for the nonlinear energy approach are presented in section 5.

Numerical results

In this section, we present new numerical computations for the linear and nonlinear stability analyses. Our analysis supports the work of Franchi et at [19] by computing the stationary convection instability threshold equation (8), and the oscillatory convection threshold equation (9). Both cases are studied by using golden section search to minimise

over a^2 and find the critical values of R^2 for linear instability. Moreover, the critical Rayleigh numbers of nonlinear energy stability Ra_E for fixed a^2 and λ is determined using equation (18). Then, we employ golden section search to minimise in a^2 and then maximise in λ to determine Ra_E, where for $R_E^2 < Ra_E$ we have stability for the best values of the coupling parameter λ. We have to do the minimization in equation (8), equation (9) and equation (18) numerically by using Matlab routines. For the parameters that are employed in this article, we have to be very careful when minimize R^2 in equation (8) and equation (9) over a^2. In all cases, we found that the stationary curve always lies below the oscillatory convection one.

In the present study, Tables 1,2 and Tables 3,4 display the numerical results for values of $\varepsilon = 0.00001$, $\varphi = 0.9999$, $\mu_1 = \mu_2 = 0.1$, $L_p = 15$ and $\Gamma_s = 0.1$ with fixed value of the inter-phase heat transfer parameter $H = 0.00001,\ 0.01$, and the porosity modified conductivity ratio $\Gamma_p = 0.1, 1$ with various values of the porosity modified interaction coefficients S_1 and S_2. We also present in Figures 1, 2 and Figures 3, 4 the critical Rayleigh number Ra which is plotted against S_1 and S_2. From Table 1, the values of ε, φ, Γ_p and H are suggested by Nield and Kuznetsov [10], it is observed that when $S_1 = 0.01$ and $\Gamma_p = 0.1$ the stationary convection boundary, $Ra_{sta} = 39.4815$, is similar to that found in Nield and Kwznetsove [10]. For an increase the value of S_1 from 0.01 to 1, the critical values of Ra_{sta} and Ra_E is increased as seen in Table1 and Table2. However, from Figures 1 and 2 we observe that as Γ_p increases from $\Gamma_p = 0.1$ to $\Gamma_p = 1$, the values of Ra are increasing this shows the stabilizing effect of the porosity modified conductivity ratio Γ_p. It is clear from Figures 1 and 2, and from Tables 1 and 2 that when $\Gamma_p = 0.1$ the stationary convection boundary Ra_{sta} decreases with increasing H, which shows the destabilizing effect. In addition, the distance between Ra_{sta} and Ra_E increases with decreasing H. Thus, with small values of H we have wide subcritical regions.

Table 3 and Table 4 show that for fixed value of Γ_p, as S_2 increases, the critical Rayleigh number increases. Thus, an increasing in S_2 causes the system becomes more stable. It is also observed that for a fixed value of Γ_p the effect of increasing the value of S_2 is to increase the critical wave number for the onset of linear instability. For example, for $\Gamma_p = 0.1$ and $S_2 = 1.01$ the critical wave number is $a_L = 11.0525$, when $S_2 = 8.01$, the critical wave number $a_L = 22.9938$. This means the cells become narrower due to the intense increasing of the critical wave number. Further, it is evident from Figures 3 and 4 that as the value of Γ_p decreases, the difference between the linear instability and nonlinear stability thresholds increases. As a result, the region of potential subcritical instabilities between the linear and nonlinear stability thresholds considerable. It is also noted that as Γ_p increases the linear instability and nonlinear stability thresholds become closer. This is, in a sense, the best

possible agreement between the two thresholds since the region of potential subcritical instabilities decreases.

Figure 5 and Table 5 display the effect of $\Gamma_s = 0.1,1$ with $\mu_1 = 0.5, 0.1$ and $\mu_2 = 0.1, 0.5$,respectively for fixed value of $S_2 = 0.01, \Gamma_p = 0.1$ and $\mathrm{H} = 0.01,$ and for various values of S_1. It is found that the effect of increasing S_1 is to increases the critical Rayleigh number Ra. However, Figure 5 shows that as Γ_s and μ_2 increase with the decreasing μ_1, Ra increases. Therefore, the parameter Γ_s have a stabilizing effect on the stability of the system. Furthermore, the effect of increasing Γ_s is to increases the value of wave number. For example, for $S_1 = 6$ and $\Gamma_s = 0.1$ we see from Table 5 that the wave number $a_L = 9.9314$, whereas, when $\Gamma_s = 1$ for the same parameter $S_1 = 6$, the wave number $a_L = 11.3416$. This indicates that the cell width decreases with increasing the parameter Γ_s, which corresponds to the narrower convection cells. It is also observed that, for a fixed value of $\mu_1 = 0.5$, $\mu_2 = 2$ and $\Gamma_s = 0.1$, the effect of increasing S_2 is to increases the wave number. For example, for $S_2 = 4$, we see from Table 6 that the wave number $a_L = 12.6119$, whereas, when $S_2 = 8$, the wave number $a_L = 15.3255$, which leads to cells becoming narrower.

Table 1-Critical Rayleigh and wave numbers of linear and energy theory, vs. S_1, for $H = 0.00001,\ \varepsilon = 0.00001,\ \varphi = 0.9999,\ \mu_1 = \mu_2 = 0.1$

$S_2 = 0.01,\ L_p = 15,\ \Gamma_s = 0.1$						
	S_1	Ra_{sta}	a_L	Ra_E	a_E	λ
$\Gamma_p = 0.1$	0.01	39.4815	9.8672	22.8990	10.3919	0.98978
	1.01	39.7958	9.6768	23.6458	10.5924	0.9901
	2.01	39.9430	9.5673	24.0238	10.6205	0.9903
	3.01	40.0281	9.4981	24.2527	10.6205	0.9903
	4.01	40.0832	9.4503	24.4060	10.5925	0.9906
	5.01	40.1219	9.4166	24.5160	10.5699	0.9905
	6.01	40.1505	9.3908	24.5986	10.5612	0.9906
	7.01	40.1725	9.3703	24.6631	10.5838	0.9906
	8.01	40.1900	9.3546	22.8990	10.3919	0.98978
$\Gamma_p = 1$	0.01	39.4966	9.8738	23.74825	10.36921	0.888371
	1.01	40.7093	10.0459	24.49263	10.58381	0.892342
	2.01	41.3136	10.0550	24.86931	10.60646	0.894236
	3.01	41.6760	10.0368	25.0972	10.60646	0.895142
	4.01	41.9175	10.0154	25.24983	10.58381	0.895356
	5.01	42.0898	9.9946	25.35915	10.56115	0.896608
	6.01	42.2190	9.9767	25.4412	10.54715	0.897087
	7.01	42.3193	9.9619	25.5050	10.53315	0.897382
	8.01	42.3995	9.9487	25.5562	10.52449	0.897647

Table 2 -Critical Rayleigh and wave numbers of linear and energy theory, vs. S_1, for $H = 0.01$,
$\varepsilon = 0.00001,\ \varphi = 0.9999,\ \mu_1 = \mu_2 = 0.1$

$S_2 = 0.01,\ L_p = 15,\ \Gamma_s = 0.1$						
	S_1	Ra_{sta}	a_L	Ra_E	a_E	λ
$\Gamma_p = 0.1$	0.01	36.69807	9.215543	22.91493	10.37787	0.989563
	1.01	37.03958	9.073001	23.66157	10.60646	0.989909
	2.01	37.19873	8.988991	24.03958	10.62912	0.990123
	3.01	37.29039	8.930459	24.26847	10.64312	0.990123
	4.01	37.34988	8.89176	24.42182	10.60646	0.990205
	5.01	37.39158	8.864721	24.53175	10.58381	0.990205
	6.01	37.42242	8.84296	24.61438	10.56115	0.990337
	7.01	37.44614	8.826617	24.67874	10.54715	0.990337
	8.01	37.46496	8.81436	24.73028	10.53315	0.990337
$\Gamma_p = 1$	0.01	39.21878	9.805174	23.76454	10.36921	0.888025
	1.01	40.42548	9.975719	24.50874	10.59246	0.891996
	2.01	41.02581	9.984855	24.88625	10.62912	0.990123
	3.01	41.38551	9.965987	25.11328	10.73909	0.895142
	4.01	41.62501	9.944595	25.26594	10.58381	0.895834
	5.01	41.79588	9.924763	25.37527	10.58381	0.896394
	6.01	41.92388	9.906491	25.45736	10.54715	0.896822
	7.01	42.02333	9.892674	25.52126	10.54715	0.897168
	8.01	42.10282	9.879452	25.57236	10.52449	0.897382

Table 3-Critical Rayleigh and wave numbers of linear and energy theory, vs. S_2, for $H = 0.00001,\ \varepsilon = 0.00001,\ \varphi = 0.9999,\ \mu_1 = \mu_2 = 0.1$

$S_1 = 0.01,\ L_p = 15,\ \Gamma_s = 0.1$						
	S_2	Ra_{sta}	a_L	Ra_E	a_E	λ
$\Gamma_p = 0.1$	0.01	39.4815	9.8672	22.8990	10.3919	0.9898
	1.01	43.9789	11.5295	22.9283	10.3779	0.9865
	2.01	51.4937	13.7849	22.9430	10.3779	0.9847
	3.01	59.3218	15.8437	22.9517	10.3779	0.9837
	4.01	67.1161	17.7086	22.9575	10.3779	0.9830
	5.01	74.8110	19.4203	22.9615	10.3779	0.9825
	6.01	82.3987	21.0078	22.9645	10.3779	0.9822
	7.01	89.8857	22.4913	22.9667	10.3692	0.9820
	8.01	97.2816	23.8909	22.9685	10.3692	0.9818
$\Gamma_p = 1$	0.01	39.4966	9.8738	23.7482	10.3692	0.8884
	1.01	40.117	10.1284	23.7820	10.3779	0.8842
	2.01	41.4161	10.5795	23.7990	10.3779	0.8822
	3.01	42.9383	11.0534	23.8092	10.3779	0.8810
	4.01	44.5496	11.5188	23.8159	10.3779	0.8801
	5.01	46.1978	11.9719	23.8206	10.3692	0.8794
	6.01	47.8594	12.4093	23.8240	10.3692	0.8791
	7.01	49.5228	12.8318	23.8266	10.3692	0.8787
	8.01	51.1819	13.2422	23.8286	10.3692	0.8785

Table 4-Critical Rayleigh and wave numbers of linear and energy theory, vs. S_2, for $H = 0.01,\ \varepsilon = 0.00001,\ \varphi = 0.9999,\ \mu_1 = \mu_2 = 0.1$

$S_1 = 0.01,\ L_p = 15,\ \Gamma_s = 0.1$						
	S_2	Ra_{sta}	a_L	Ra_E	a_E	λ
$\Gamma_p = 0.1$	0.01	36.6980	9.2155	22.9149	10.3779	0.9896
	1.01	41.7939	11.0525	22.9442	10.3919	0.9862
	2.01	49.3713	13.2610	22.9590	10.3919	0.9845
	3.01	57.1666	15.2537	22.9677	10.3919	0.9834
	4.01	64.9004	17.0529	22.9735	10.3919	0.9828
	5.01	72.5255	18.6989	22.9775	10.3919	0.9823
	6.01	80.0404	20.2252	22.9805	10.3919	0.9819
	7.01	87.4544	21.6503	22.9827	10.3779	0.9816
	8.01	94.7780	22.9938	22.9844	10.3779	0.9814
$\Gamma_p = 1$	0.01	39.2188	9.8052	23.7645	10.3692	0.8880
	1.01	39.8485	10.0617	23.7984	10.3919	0.8840
	2.01	41.1489	10.5122	23.8154	10.3919	0.8819
	3.01	42.6696	10.9826	23.8255	10.3919	0.8807
	4.01	44.2780	11.4461	23.8322	10.3779	0.8798
	5.01	45.9226	11.8951	23.8369	10.3779	0.8792
	6.01	47.5804	12.3303	23.8403	10.3779	0.8789
	7.01	49.2397	12.7503	23.8429	10.3779	0.8785
	8.01	50.8946	13.1566	23.8449	10.3779	0.8782

Table 5-Critical Rayleigh and wave numbers of linear and energy theory, vs. S_1, for $S_2 = 0.01\ \varepsilon = 0.00001,\ \varphi = 0.9999,\ \Gamma_s = 0.1,1$

$H = 0.01,\ L_p = 15,\ \Gamma_p = 0.1$						
	S_1	Ra_{sta}	a_L	Ra_E	a_E	λ
$\mu_1 = 0.5$ $\mu_2 = 0.1$ $\Gamma_s = 0.1$	1.01	40.4902	9.9940	24.6603	10.5838	0.8783
	2.01	41.0995	10.0057	25.0361	10.6065	0.8805
	3.01	41.4648	9.9883	25.2633	10.6065	0.8818
	4.01	41.7081	9.9666	25.4152	10.5838	0.8829
	5.01	41.8818	9.9471	25.5238	10.5612	0.8835
	6.01	42.0119	9.9314	25.6052	10.5471	0.8840
	7.01	42.1130	9.9150	25.6683	10.5245	0.8844
	8.01	42.1938	9.9018	25.7188	10.5245	0.8854
$\mu_1 = 0.1$ $\mu_2 = 0.5$ $\Gamma_s = 1$	1.01	41.0188	10.2211	33.5235	10.8351	0.9193
	2.01	42.6773	10.5575	34.8189	11.1823	0.9225
	3.01	44.1767	10.8250	35.9930	11.4702	0.9253
	4.01	45.5436	11.0377	37.0659	11.6934	0.9275
	5.01	46.7979	11.2067	38.0525	11.8767	0.9295
	6.01	47.9551	11.3416	38.9645	12.0320	0.9313
	7.01	49.0273	11.4480	39.8112	12.1506	0.9328
	8.01	50.0243	11.5305	40.6000	12.2466	0.9342

Table 6- Critical Rayleigh and wave numbers of linear and energy theory, vs. S_2, for $S_1 = 0.01$
$\varepsilon = 0.00001,\ \varphi = 0.9999,\ \Gamma_s = 0.1,1$

$H = 0.01,\ L_p = 15,\ \Gamma_p = 0.1$						
	S_2	Ra_{sta}	a_L	Ra_E	a_E	λ
$\mu_1 = 0.5$ $\mu_2 = 2$ $\Gamma_s = 0.1$	1.01	40.4870	10.3061	32.8520	10.3552	0.8616
	2.01	42.6969	11.0707	32.8797	10.3552	0.8593
	3.01	45.2245	11.8548	32.8946	10.3552	0.8579
	4.01	47.8633	12.6119	32.9031	10.3552	0.8572
	5.01	50.5382	13.3353	32.9078	10.3412	0.8568
	6.01	53.2175	14.0272	32.9102	10.3412	0.8564
	7.01	55.8869	14.6913	32.9110	10.3412	0.8563
	8.01	58.5396	15.3255	32.9107	10.3326	0.8563
$\mu_1 = 0.2$ $\mu_2 = 0.05$ $\Gamma_s = 1$	1.01	39.3037	9.8505	25.8696	10.3919	0.8931
	2.01	39.5780	9.9742	25.9125	10.4059	0.8882
	3.01	39.9777	10.144	25.9520	10.4145	0.8836
	4.01	40.4714	10.3442	25.9884	10.4285	0.8794
	5.01	41.0363	10.5642	26.0221	10.4372	0.8756
	6.01	41.6559	10.7979	26.0533	10.4512	0.8720
	7.01	42.3178	11.0387	26.0824	10.4512	0.8686
	8.01	43.0127	11.2847	26.1096	10.4512	0.8656

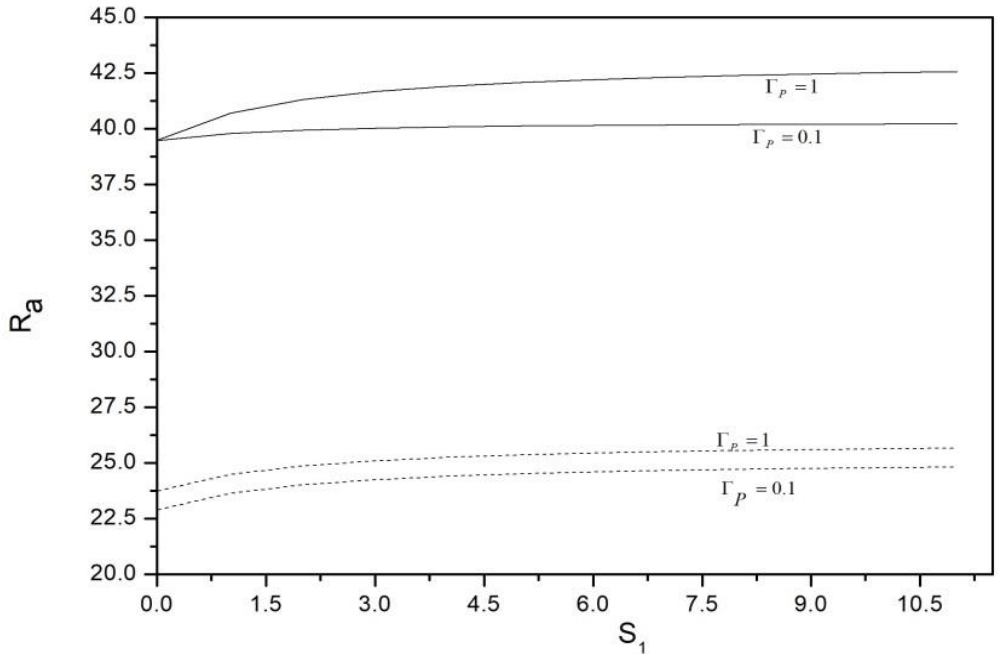

Figure 1-Critical Rayleigh number Ra is plotted against S_1 with $\varepsilon = 0.00001,\ \varphi = 0.9999,$ $\Gamma_s = 0.1,\ L_p = 15, S_2 = 0.01.$ The solid curves are for linear instability and the dotted curves are for nonlinear stability, for $\Gamma_p = 0.1, 1, H = 0.00001,$, and $\mu_1 = \mu_2 = 0.1$.

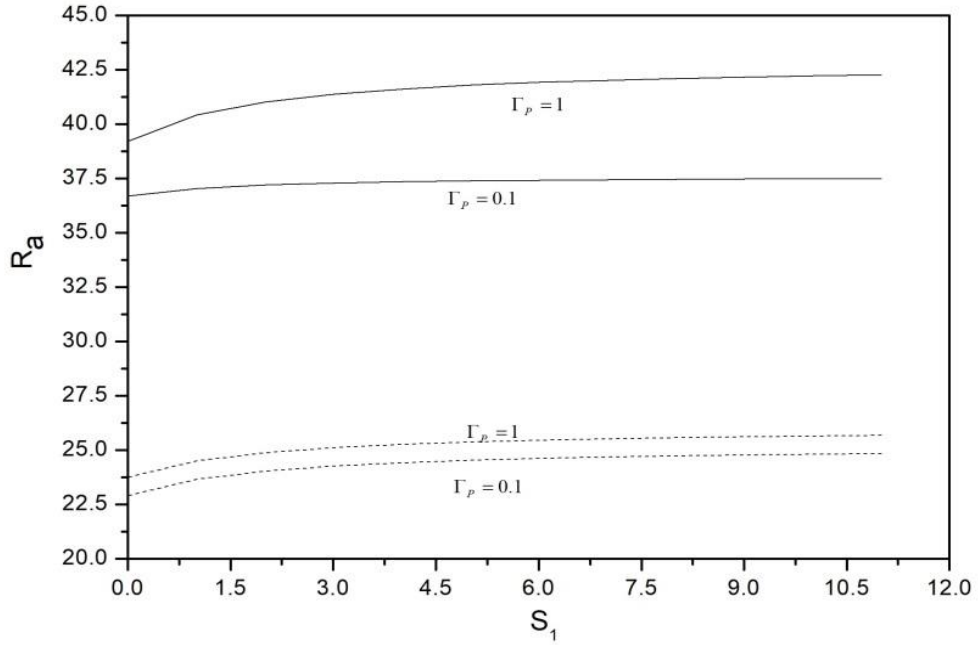

Figure 2-Critical Rayleigh number Ra is plotted against S_1 with $\varepsilon = 0.00001,\ \varphi = 0.9999,$ $\Gamma_s = 0.1,\ L_p = 15,\ S_2 = 0.01.$ The solid curves are for linear instability and the dotted curves are for nonlinear stability, for $\Gamma_p = 0.1, 1,\ H = 0.01,$ and $\mu_1 = \mu_2 = 0.1.$

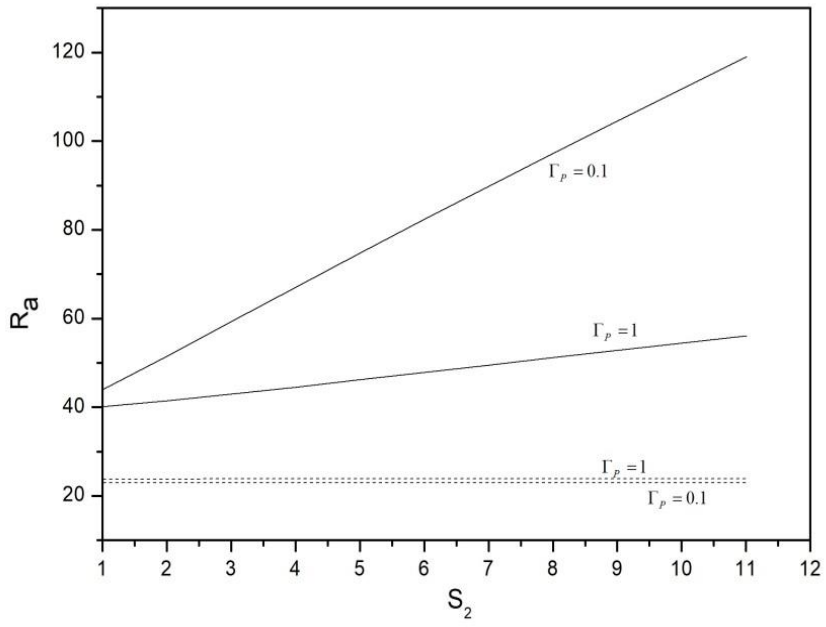

Figure 3-Critical Rayleigh number Ra is plotted against S_2 with $\varepsilon = 0.00001,\ \varphi = 0.9999,$ $\Gamma_s = 0.1,\ L_p = 15,\ S_1 = 0.01.$ The solid curves are for linear instability and the dotted curves are for nonlinear stability, for $\Gamma_p = 0.1, 1, H = 0.00001,$, and $\mu_1 = \mu_2 = 0.1.$

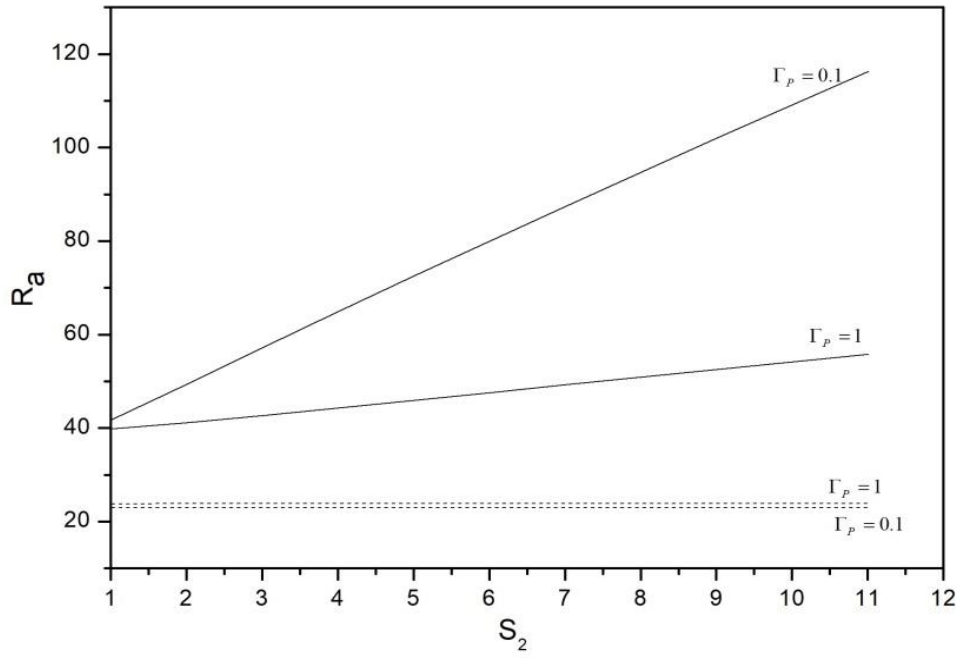

Figure 4-Critical Rayleigh number Ra is plotted against S_2 with $\varepsilon = 0.00001,\ \varphi = 0.9999,$ $\Gamma_s = 0.1,\ L_p = 15,\ S_1 = 0.01$. The solid curves are for linear instability and the dotted curves are for nonlinear stability, for $\Gamma_p = 0.1, 1, H = 0.01,$ and $\mu_1 = \mu_2 = 0.1$.

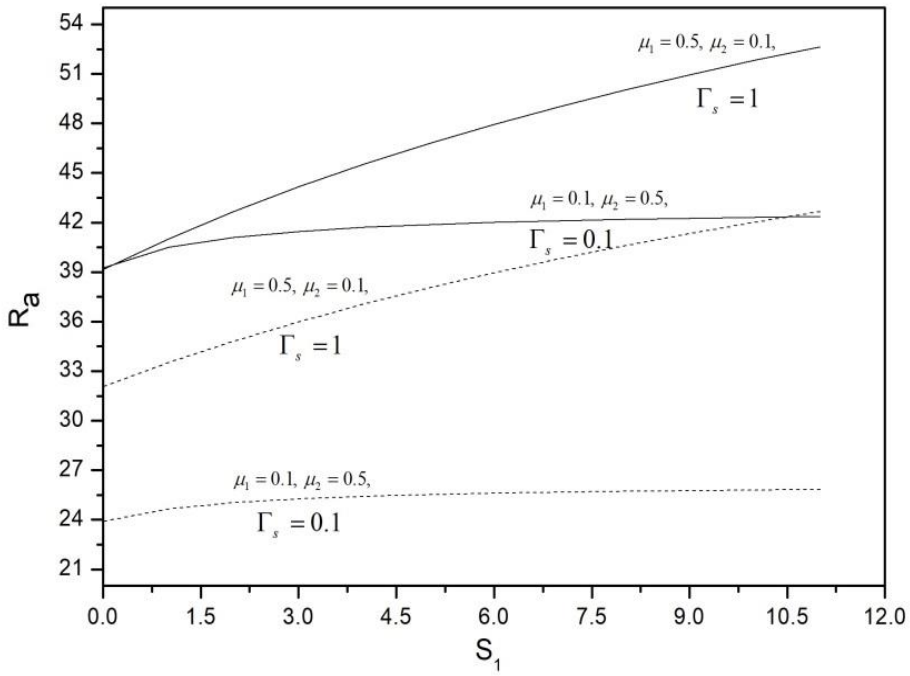

Figure 5-Critical Rayleigh number Ra is plotted against S_1 with $\varepsilon = 0.00001,\ \varphi = 0.9999,$ $\Gamma_p = 0.1,\ L_p = 15,\ S_2 = 0.01$. The solid curves are for linear instability and the dotted curves are for nonlinear stability, for $\Gamma_p = 0.1, 1, H = 0.01$.

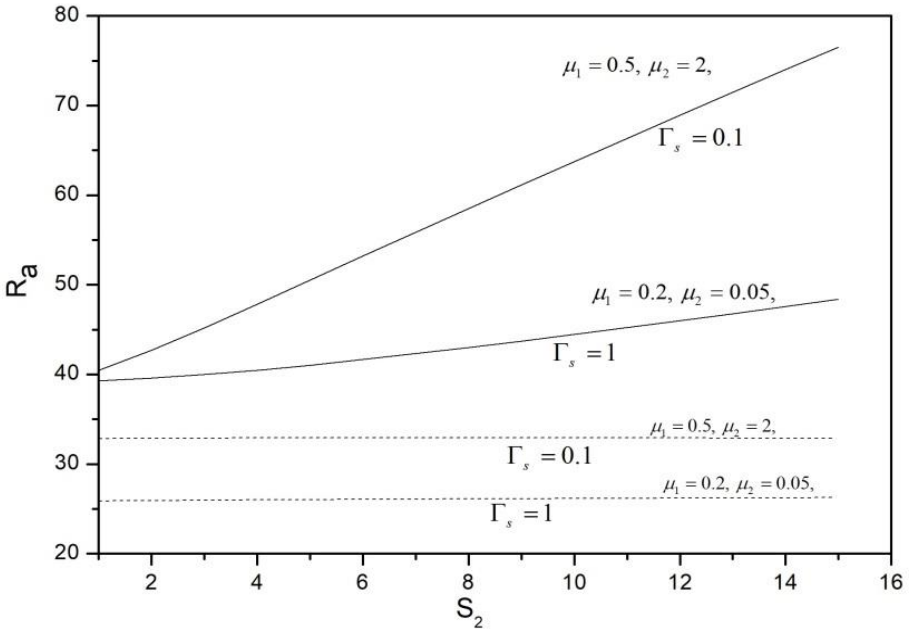

Figure 6-Critical Rayleigh number Ra is plotted against S_2 with $\varepsilon = 0.00001,\ \varphi = 0.9999,$ with $\Gamma_p = 1,\ L_p = 15, S_1 = 0.01$. The solid curves are for linear instability and the dotted curves are for nonlinear stability, for $\Gamma_p = 0.1, 1, H = 0.01$.

Conclusion

The onset of convection in a fluid saturated bidsperse porous medium is investigated when the temperature of the fluid and solid phases is in local thermal non-equilibrium. The linear instability threshold and nonlinear one is derived analytically in case of free surfaces. The stationary convection boundary, $\boldsymbol{Ra_{sta} = 39.4815,}$ is similar to that found by Nield and Kwznetsove for particular values of the porosity modified interaction coefficient and the porosity modified conductivity ratio, $\boldsymbol{\varepsilon = 0.00001}$, $\boldsymbol{\varphi = 0.9999}$, $\boldsymbol{H = 0.00001}$, $S_2 = 0.01,\ L_p = 15,\ \Gamma_s = 0.1$ and $\boldsymbol{\Gamma_p = 0.1}$. Through investigation we found that the onset of convection is by stationary convection for various interaction parameters. It can be argued from the results that the critical Rayleigh numbers Ra and the critical wave numbers a_L are greater in the case of $\boldsymbol{\mu_1 = \mu_2 = 0.1, L_p = 15}$ and $\boldsymbol{S_2}$ increases. Also, we observed that the subcritical instability region decreases as the parameter $\boldsymbol{\Gamma_s}$ increases. The effects of increasing $\boldsymbol{\Gamma_p}$ and $\boldsymbol{\Gamma_s}$ as well as increasing the value of $\boldsymbol{S_1}$ were seen to stabilize the system. Also, we observed that for small values of $\boldsymbol{\Gamma_p}$ and $\boldsymbol{\Gamma_s}$, the effect of increasing $\boldsymbol{S_2}$ is to stabilize the system. This indicates that the thermal convection occurs more easily.

References

[1] Szczygieł, J., **2006.** Enhancement of reforming efficiency by optimizing the porous structure of reforming catalyst, Theoretical considerations *Fuel*, 85 1579–1590.

[2] Lin, F. C. ,Liu, B. H. ,Juan, C. C. and Chen, Y. M., **2011**. Effect of pore size distribution in bidisperse wick on heat transfer in a loop heat pipe, *Heat and mass transfer*, 47 933-940.

[3] Shi ,J. Q. and Durucan, S., **2005** .Gas storage and flow in coalbed reservoirs: Implementation of a bidisperse pore model for gas diffusion in a coal matrix SPE Res. Eval. ,and Eng. 8 169–175.

[4] Nield, D. A. and Bejan, A., **2017**. Convection in Porous Media Springer New York.

[5] Straughan, B., **2015**. Convection with local thermal non-equilibrium and microfluidic effects Springer.

[6] Nield, D. A. and Kuznetsov, A. V., **2004**. Forced convection in a bi-disperse porous medium channel:a conjugate problem *Int. J. Heat Mass Transfer*, 47 5375-5380.
[7] Nield, D. A. and Kuznetsov, A. V., **2005**. A two-velocity two-temperature model for a bi-dispersed porous medium: Forced convection in a channel. *Transp. Porous Media,* 59 325-339.
[8] Nield, D. A. and Kuznetsov, A. V., **2006**. The onset of convection in a bidisperse porous medium *Int. J. Heat Mass Transfer*, 49 3068-3074.
[9] Nield, D. A. and Kuznetsov, A. V., **2007**. The effect of combined vertical and horizontal heterogeneity on the onset of convection in a bidisperse porous medium *Int. J. Heat Mass Transfer*, 50 3329-3339.
[10] Nield D A and Kuznetsov A V., 2008. Natural convection about a vertical plate embedded in a bidisperse porous medium *Int. J. Heat Mass Transfer* 51 1658-1664.
[11] Nield, D. A. and Kuznetsov, A. V., **2013**. A note on modeling high speed flow in a bidisperse porous medium, *Transp. Porous Media* 96 495-499.
[12] Gentile, M. and Straughan, B., **2017**. Bidispersive thermal convection *Int. J. Heat Mass Transfer*, 114 837-840.
[13] Gentile, M. and Straughan, B., **2017**. Bidispersive vertical convection, *Proc. R. Soc. A* 473 20170481.
[14] Straughan, B., **2018**. Horizontally isotropic bidispersive thermal convection *Proc. R. Soc. A*, 474 20180018.
[15] Straughan, B., **2018**. Bidispersive double diffusive convection *Int. J. Heat Mass Transfer*, 126 504-508.
[16] Straughan, B., **2019**. Horizontally isotropic double porosity convection *Proc. R. Soc. A,* 475 20180672.
[17] Straughan, B .**2019.** Effect of inertia on double diffusive bidispersive convection *Int. J. Heat Mass Transfer*, 129 389-396.
[18] Saleh, H. and Haddad, S.A., **2020**. Effect of anisotropic permeability on double-diffusive bidisperse porous medium *Heat Transfer*, 49 1825-1841.
[19] Franchi, F., Nibbi , R. and Straughan, B., **2017**. Modelling bidispersive local thermal non-equilibrium flow *Fluids* ,2 48.
[20] Malashetty, M. S ., Shivakumara, I .S. and Kulkarni, S., **2005** .The onset of Lapwood–Brinkman convection using a thermal non- equilibrium model *Int. J. Heat Mass Transfer*, 48 1155-1163.
[21] Malashetty, M .S ., Shivakumara, I. S. and Kulkarni, S., **2005**. The onset of convection in an anisotropic porous layer using a thermal non-equilibrium model. *Transp. Porous Media,* 60 199-215.
[22] Shivakumara, I. S., Malashetty, M. S. and Chavaraddi, K. B., **2006** . Onset of convection in a viscoelastic-fluid-saturated arselypacked porous layer using a thermal nonequilibrium model *Can. J. phys*. 84 973-990.
[23] Straughan, B .,**2006**. Global nonlinear stability in porous convection with a thermal non-equilibrium model *Proc. R. Soc. A* , 462 409-418.
[24] Malashetty, M. S., Swamy, M. and Kulkarni, S., **2007**. Thermal convection in a rotating porous layer using a thermal nonequilibrium model *Phys. Fluids*, 19 (5) 054102.
[25] Malashetty, M.S. Heera, R. ,**2008**. Linear and non-linear double diffusive convection in a rotating porous layer using a thermal non-equilibrium model *Int. J. Non Linear Mech.* 43 600-621.
[26] Malashetty, M. S., Swamy, M. and Heera, R. ,**2008**. Double diffusive convection in a porous layer using a thermal non- equilibrium Model, *Int. J. Therm. Sci*. 47 1131-1147.
[27] Malashetty, M. S., Shivakumara, I. S. and Kulkarni, S., **2009**. The onset of convection in a couple stress fluid saturated porous layer using a thermal non-equilibrium model *Phys. Lett. A,* 373 781-790.
[28] Gaikwad, S. N., Malashetty, M. S. and Prasad, K. R. **2009**. Linear and non-linear double diffusive convection in a fluid-saturated anisotropic porous layer with cross-diffusion effects *Transp. Porous Media* , 80 37-560.
[29] Malashetty, M. S. and Swamy, M., **2010**. Effect of rotation on the onset of thermal convection in a sparsely packed porous laye using a thermal non-equilibrium model, *Int. J. Heat Mass Transfer*, 53 3088-3101.

[30] Shivakumara, I .S ., Mamatha, A. L. and Ravisha, M.,**2010**. Effects of variable viscosity and density maximum on the onset of Darcy-Bénard convection using a thermal nonequilibrium model *J. Porous Media,* 13 .

[31] Shivakumara, I .S., Lee, J., Vajravelu, K. and Mamatha, A. L.,**2011**. Effects of thermal nonequilibrium and non-uniform temperature gradients on the onset of convection in a heterogeneous porous medium *Int. Commun. Heat Mass Transfer,* 38 906-910.

[32] Barletta, A. and Celli, M. ,**2011**. Local thermal non-equilibrium flow with viscous dissipation in a plane horizontal porous Layer *Int J. Therm. Sci*. 50 53-60.

[33] Straughan, B. **2013**. Porous convection with local thermal non-equilibrium temperatures and with Cattaneo effects in the solid, *Proc. R. Soc. A,* 469 20130187.

[34] Dayananda, R. N. and Shivakumara, I. S., **2019**. Impact of thermal non-equilibrium on weak nonlinear rotating porous convection *Transp. Porous Media,* 130 819-845.

[35] Santamaria-Holek, I., Grzywna, Z. J. and Rubi, J. M. **2012**. A non-equilibrium thermodynamics model for combined adsorption and diffusion processes in micro- and nanopores *J. Non-Equilib. Thermodyn,* 37 273–290.

[36] Al-Hhafajy, D.G.S. and Abdulhadi, A., **2014**. Magnetohydrodynamic Peristaltic flow of a couple stress with heat and mass transfer of a Jeffery fluid in a tube through porous medium. *Advances in Physics Theories and Applications, IISTE, 32,* pp.16-42.

[37] Al-Khafajy, D.G.S. and Labban, J.A., **2021**. Temperature and Concentration Effects on Oscillatory Flow for Variable Viscosity Carreau Fluid through an Inclined Porous Channel. *Iraqi Journal of Science*, pp.45-53.

[38] Kareem, R.S. and Abdulhadi, A.M., **2020**. Impacts of Heat and Mass Transfer on Magneto Hydrodynamic Peristaltic Flow Having Temperature-dependent Properties in an Inclined Channel Through Porous Media. *Iraqi Journal of Science*, pp.854-869.

[39] Khudair, W.S. and Al-Khafajy, D.G.S., **2018**. Influence of heat transfer on Magneto hydrodynamics oscillatory flow for Williamson fluid through a porous medium. *Iraqi Journal of Science*, *59*(1B), pp.389-397.

[40] Haddad, S. A., **2014**. Thermal convection in a Darcy porous medium with anisotropic spatially varying permeability *Acta Appl. Math*.132 359-370.

[41] Haddad, S. A., **2017**. Thermal convection in a rotating anisotropic fluid saturated Darcy porous medium *Fluid,* 2 44.

[42] Chandrasekhar, S., **2013**. Hydrodynamic and hydromagnetic stability Courier Corporation.